

Magnetic Causes of the Eruption of a Quiescent Filament

B. Schmieder · V. Bommier · R. Kitai · T. Matsumoto ·
T.T. Ishii · M. Hagino · H. Li · L. Golub

Received: 10 July 2007 / Accepted: 27 November 2007 / Published online: 25 December 2007
© Springer Science+Business Media B.V. 2007

Abstract During the JOP178 campaign in August 2006, we observed the disappearance of our target, a large quiescent filament located at S25°, after an observation time of three days (24 August to 26 August). Multi-wavelength instruments were operating: THEMIS/MTR (“MulTi-Raies”) vector magnetograph, TRACE (“Transition Region and Coronal Explorer”) at 171 Å and 1600 Å and Hida Domeless Solar telescope. Counter-streaming flows ($\pm 10 \text{ km s}^{-1}$) in the filament were detected more than 24 hours before its eruption. A slow rise of the global structure started during this time period with a velocity estimated to be of the order of 1 km s^{-1} . During the hour before the eruption (26 August around 09:00 UT) the velocity reached 5 km s^{-1} . The filament eruption is suspected to be responsible for a slow CME observed by LASCO around 21:00 UT on 26 August. No brightening in H α or in coronal lines, no new emerging polarities in the filament channel, even with the high polarimetry sensitivity of THEMIS, were detected. We measured a relatively large decrease of the photospheric magnetic field strength of the network (from 400 G to 100 G), whose downward magnetic tension provides stability to the underlying

Electronic supplementary material The online version of this article (<http://dx.doi.org/10.1007/s11207-007-9100-9>) contains supplementary material, which is available to authorized users.

B. Schmieder (✉)
Observatoire de Paris, LESIA, CNRS UMR 8109, 92195 Meudon Cedex, France
e-mail: brigitte.schmieder@obspm.fr

V. Bommier
Observatoire de Paris, LERMA, CNRS UMR 8112, 92195 Meudon Cedex, France
e-mail: veronique.bommier@obspm.fr

R. Kitai · T. Matsumoto · T.T. Ishii · M. Hagino
Hida Observatory, University of Kyoto, Kyoto, Japan

H. Li
Purple Mountain Observatory, Nanjing 210008, China

L. Golub
Harvard-Smithsonian Center for Astrophysics, Cambridge, MA 02138, USA

stressed filament magnetic fields. According to some MHD models based on turbulent photospheric diffusion, this gentle decrease of magnetic strength (the tension) could act as the destabilizing mechanism which first leads to the slow filament rise and its fast eruption.

Keywords Sun: filament, eruption · Magnetic field

1. Introduction

Disappearance of filaments and subsequent coronal mass ejections (CMEs) have often been observed with SOHO, and statistical studies (Subramanian and Dere, 2001) indicate that 45% of CMEs are produced by filament eruptions related to flares and 15% by filaments with no flare association. The disappearance of filaments can be of thermal nature (Mouradian, Martres, and Soru-Escout, 1986) or of dynamic nature (Démoulin and Vial, 1992) or both in the case of two ribbon flares (Schmieder *et al.*, 2006). The global magnetic strength surrounding prominences and the amount of free magnetic energy play an important role in the evolution of activated filaments (Švetska, 1986). Although a number of studies (see reviews of Wang, 2002; Schmieder and van Driel-Gesztelyi, 2005) have given some insights into the physical quantities which cause CME initiation, for filament eruptions the triggering process is still unclear. On the other hand we have a better understanding of the magnetic configuration of filaments due to recent 3D magnetic modeling of filaments following the work of Aulanier and Démoulin (1998). The filament can be represented by a twisted flux rope in a bipolar magnetic background and the parasitic polarities in the filament channel can be responsible for the existence of the lateral feet of the prominence (Dudík *et al.*, 2007). The role of minor polarities in the filament channel seems to be crucial in filament disappearance. Canceling flux was suggested to be responsible for filament eruption (Schmieder *et al.*, 2000; Schmieder *et al.*, 2002) and identified for the partial filament disappearance process (Schmieder *et al.*, 2006; Zhou, Wang, and Cao, 2003). Flux cancelation could occur when opposite polarities converge towards the inversion line, or if minor polarities of one sign are transported through the magnetic inversion line in the filament channel towards the region of opposite sign and then cancel with some polarities (Lin *et al.*, 2005; Rondi *et al.*, 2007). Shearing motions were predicted to also be an important factor, but it is still difficult to observe such a slow evolution of the magnetic field. A recent attempt was made using the helioseismology (Hindman, Haber, and Toomre, 2006). MacKay and van Ballegooijen (2006) suggested an evolution in two or three days for the detection of shearing motions due to differential rotation. New emerging flux would be associated with an active generation of currents by photospheric motions (Kuin, Paul, and Martens, 1986). This could increase the twisting current of the filament directly producing the observed rotational motion and also tending to destabilize it with respect to kink instabilities (Török, Kliem, and Titov, 2004). A nonlinear development of kink instability would restructure the magnetic field and may be the cause of upward motions and in favor of filament eruption.

An alternate explanation of the triggering mechanism may be provided in the context of some coronal reconnection above or below the flux rope (breakout or tether-cutting) (Antiochos, DeVore, and Klimchuk, 1999). Some observations appear to imply the presence of such mechanisms (Sterling and Moore, 2003). Flare-like brightenings occurring beneath the rising prominence may correspond to the “tether cutting” magnetic reconnection. The magnitude of the brightening depends on the ratio between magnetic energy and heating energy. Magnetic energy has been studied in order to determine the overall nonpotentiality of active regions (twist and shear in the magnetic field) which is primordial for eruptions as noted

above. Different proxies have been used, mainly the longitudinal magnetic field (Falconer *et al.*, 1997) or for the stronger shear the transverse field (Falconer, 2001).

Other theoretical models of eruptions are based on loss of equilibrium. In fact reconnection is not a necessary condition for eruptive prominences, which can result directly from instabilities leading to loss of equilibrium in the relevant magnetic structures (Lin, Forbes, and Isenberg, 2001; Lin and Forbes, 2000; Low, 2001). In principle, disruption occurring in a magnetic structure results from the interaction between the current and the magnetic field in the relevant configuration. A CME ejects not only the plasma but also the stressed magnetic structure which is associated with the electric current concentration that contains the mass prior to the eruption. This could be quantified by the magnetic helicity parameter which has been well studied (review Démoulin, 2007). In the loss of equilibrium models, the free energy stored in a stressed magnetic structure prior to the eruption depends on the strength of the background field. The stronger the background field is, the more free energy can be stored and thus the more energetic the eruptive process is (Lin, 2004). With a rough estimate, Lin (2004) concluded that a catastrophic loss of equilibrium in the system can be prevented if the strength of the background field is lower than 27 G (17 G in the paper of Isenberg, Forbes, and Démoulin (1993) taking into account the effect of gravity). Instead the system will evolve smoothly in response to the slow change in the boundary conditions.

During a campaign involving ground-based observations (THEMIS vector magnetograph) and space instruments (SOHO/LASCO and MDI, TRACE) we observed the eruption of a long filament. No real signatures of heating were detected in H α and in coronal lines. The complex LASCO CME is interpreted as due to the interaction of a slow CME and a fast CME triggered by a flare occurring in active region NOAA 10905 in the vicinity of the filament two hours later (ten degrees north). The origin of the slow CME could correspond to the eruption of the filament. We were able to study the evolution of magnetic strength of the background field prior to the eruption using THEMIS vector magnetic field measurements. We discuss in the last section how decreasing background field could be responsible of the destabilization of the filament. Its eruption could be due to loss of equilibrium of the flux tube, which is less and less tied in the photosphere.

2. Observations

The following data have been used in this study and are presented in movies with this paper (see the web sites indicated at the end of the paper):

1. H α survey by the Optical Solar Patrol Network (OSPAN) for 24 and 25 August 2006 by the SMART telescope in Hida and spectroheliograms in H α obtained in Meudon for the next days. OSPAN replaces the ISOON network.
2. Polarimetric data with high sensitivity obtained by THEMIS/MTR (multiline observations) for 24, 25, and 26 August 2006 (Table 1) and computed in the Fe I 6302 Å line using UNNOFIT code (Bommier *et al.*, 2007).
3. TRACE 171 Å images. TRACE (Handy *et al.*, 1999) was observing in 1600 Å and white light with a 1 min cadence and in 171 Å with a 7 min cadence. There is a gap in the observations from 00:00 UT to 04:00 UT on 26 August 2006.
4. Hida Domeless Solar Telescope (DST), H α filtergrams.

A large filament located at S25° was the target of JOP 178 for a few days before its complete disappearance on 27 August (Figure 1). It was located in a complex environment, surrounding the southern part of an active region (NOAA 10905) which crossed central

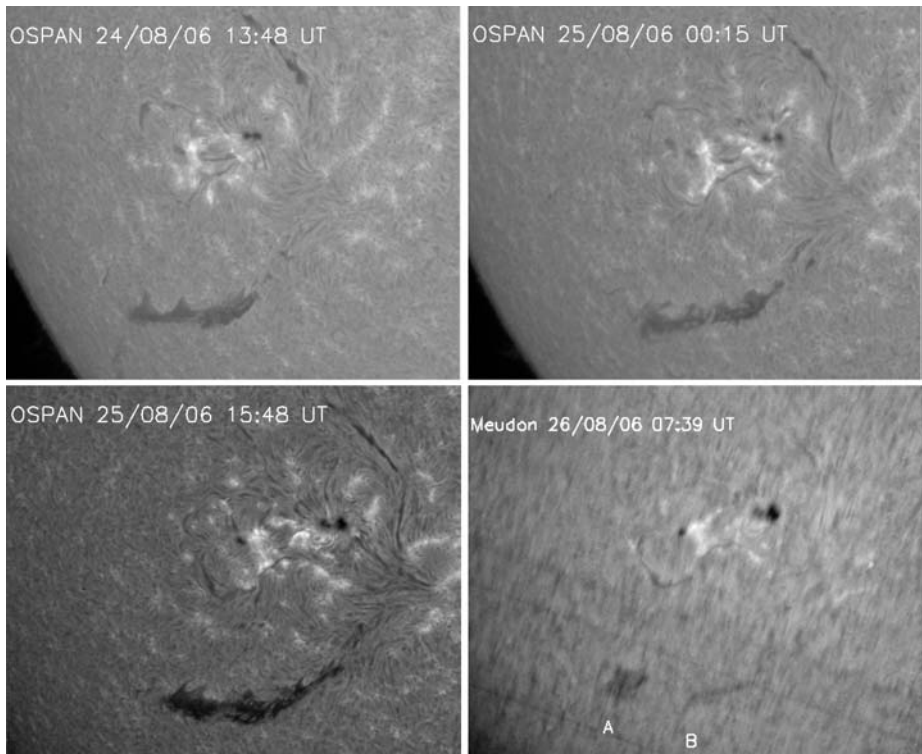


Figure 1 OSPAN $H\alpha$ observations at Big Bear Observatory for 24 August 2006 at 13:48 UT, and for 25 August 2006 at 00:15 UT and 15:48 UT (courtesy K.S. Balasubramaniam) and Meudon $H\alpha$ spectroheliogram on 26 August 2006. A large part of the filament between A and B is disappearing.

meridian on 27 August. From 25 August 2006 to 3 September 2006, Hida DST was observing and tracking filament formation and eruption. The Sun's activity was very low during this time period except for the occurrence of a C2.5 flare on 26 August at 19:52 UT in active region NOAA 10905 located N10, included in the same global magnetic configuration as the filament target.

On 26 August at 07:39 UT, in Meudon spectroheliograms, only two sections of the large filament were still present, A and B. The central part (B) of the filament was very weak and later disappeared. During the filament disappearance, the filament material seemed to be lost by sliding down to the lower layers in cool form, not to be heated to coronal temperatures. However, we can distinguish long, bright threads towards the west in the TRACE 171 Å images. Hida survey observed until 08 UT on 26 September. The eruption occurred after 09:00 UT according to TRACE observations, with part B escaping from the field-of-view around that time. On 27 August only part A of the filament remained.

3. Dynamics of the Filament

3.1. Horizontal Flows of the Prominence Plasma

This filament was a large, quiescent filament similar to that studied by Lin, Wiik, and Engvold (2003) and had similar counter-streaming flows for a long time before its eruption.

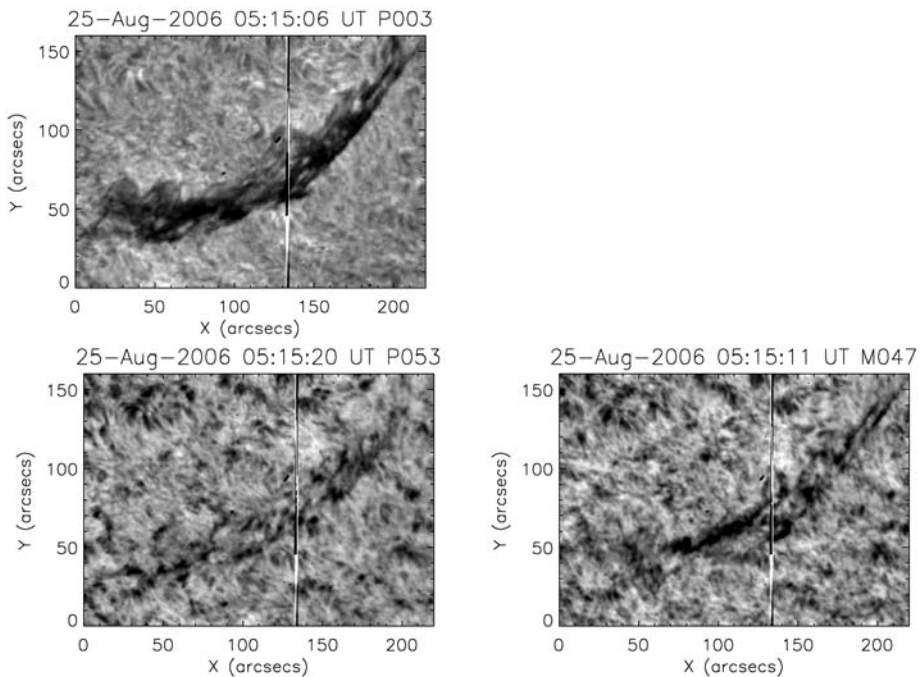


Figure 2 Hida observations of the filament on 25 August 2006 in $H\alpha$ line center, $+0.53 \text{ \AA}$ (lower left panel) and -0.47 \AA (lower right panel).

Counter-streaming flows were discovered by Zirker, Engvold, and Martin (1998), but not necessarily associated with some activity. Streaming motions were observed intermittently on 25 August. Prominent counter-streaming flows were observed on 25 August in $H\alpha$ between 0 and 8 UT (DST Hida). Counter-streaming flows also were observed on 25 August in 171 \AA (TRACE movies). We detected more flows going towards the west than to the east in the 25 August movie. On 26 August, according to the TRACE 171 \AA movie, it is not certain if counter-streaming still existed. Is counter-streaming flows a sign of a future eruption for such quiescent filaments? More observations are needed to answer this question.

3.2. Measurement of the Transverse Velocity and Dopplershifts

The high-resolution time series of Hida/DST observations allows us to continuously track the motion of absorbing features. We applied the so-called “time-slice diagram” technique to map flow directions and velocities in the filament; in both wings different structures are identified revealing the existence of counter-streamings (Figure 2). This technique was developed for filaments by Lin, Wiik, and Engvold (2003). The Hida movie of the $H\alpha$ filament observed in both wings ($\pm 0.5 \text{ \AA}$) reveals the dynamics of the small structures during three hours on 25 August 2006. To create a “time-slice diagram” we follow these points. We identified the direction of moving structures in the wings, rotated the image in that direction and cut the images in parallel slices (Figure 3). We selected a thin slice from an image along the trajectory of a moving feature to be measured, and identical slices at the same position from all the images in the time series and stacked the slices side by side with

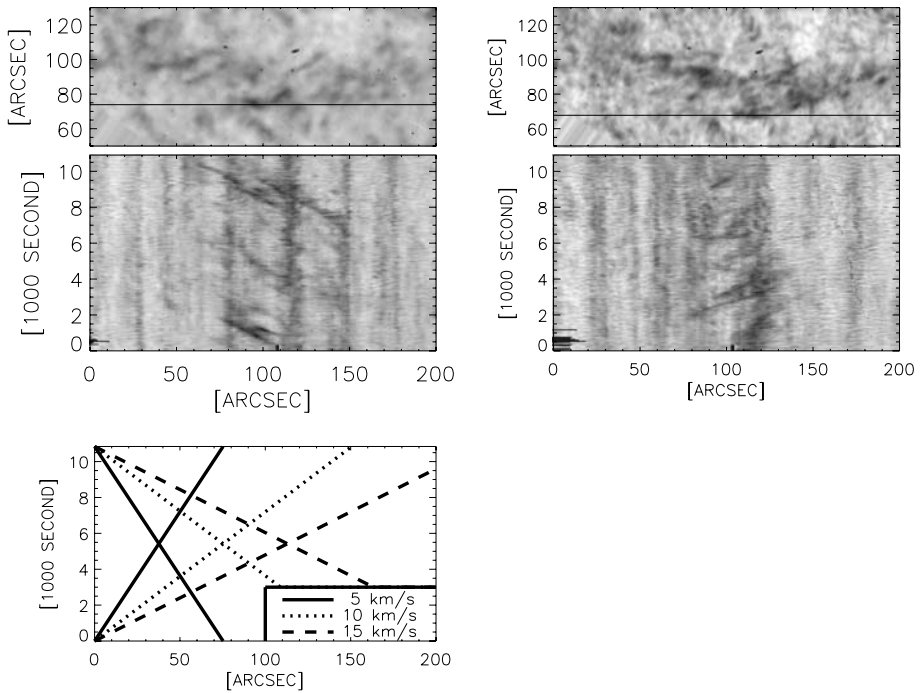


Figure 3 Transverse velocities using the time slice technique. Top panels: on the left, the rotated image in the red wing, on the right in the blue wing, the studied slice is shown by the black line. Middle panels: time slice diagrams of one slice representing the transverse velocity and the flow (downflow in the red wing and upflow in the blue wing), the slope represents the transverse velocity. Bottom panel: the calibrated slopes (negative and positive velocities).

time going from left to right (Figure 3, middle). The motions of small-scale structures in the direction of the slice will appear as inclined features in the time-slice diagrams. Because of the horizontal and vertical axes representing time and distance, respectively, the slope of the inclined feature gives the transverse velocity and the direction in the plane of the sky.

By using the time-slice technique with the DST data (see also the DST movies), transverse velocities are measured and evaluated to be of the order of $\pm 10 \text{ km s}^{-1}$.

Downflows (upflows) are represented in the red (blue) wing in the diagrams. It appears that some fine structures are red-shifted while the other ones are blue-shifted. We do not have the observations in the extreme west feet of the filament to confirm the sliding down of the plasma suggested in the TRACE movies.

3.3. Global Rise of the Magnetic Structure of the Filament

TRACE 171 \AA images allow us to follow the evolution of the filament structures. The $H\alpha$ fine structures are visible in these images due to the absorption mechanism of the Lyman continuum of He II at the 171 \AA wavelength (Mein *et al.*, 2001; Anzer and Heinzel, 2005). The optical thicknesses of $H\alpha$ and He II continuum are equivalent at this wavelength, thus the fine structures in $H\alpha$ and those visible in absorption in 171 \AA are similar (Schmieder *et al.*, 2004). In Figure 4a, b we can distinguish the fine structures in the region indicated by the letter “B” and the global pattern of a few footpoints and the filament channel represented

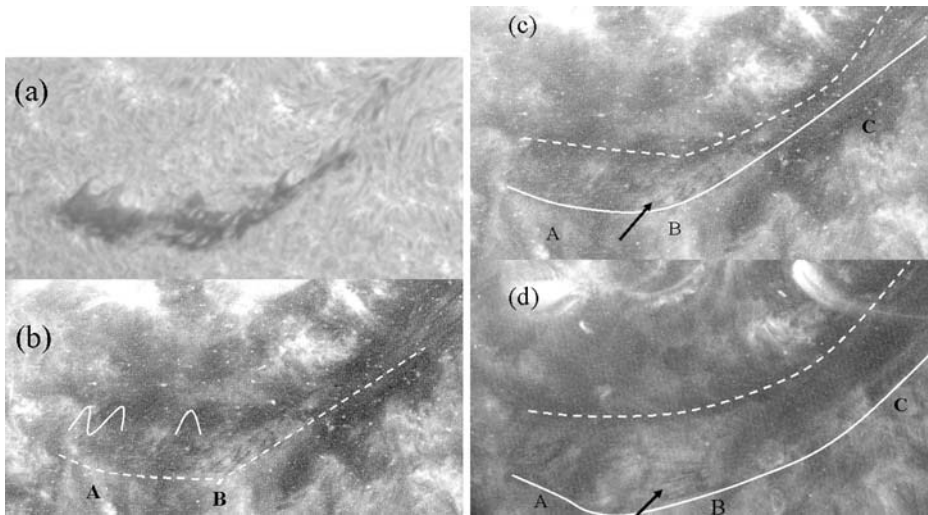


Figure 4 Filament observations on 25 August 2006 (a) in $H\alpha$ at 15:48 UT, (b) in 171 \AA at 13:04 UT. The dashed line underlines the filament spine, the continuous line the filament footpoints. The filament body lies between the dashed line and the feet. Tiny dark regions above point B represent the $H\alpha$ fine structures because of the absorption of Lyman continuum of He II at 171 \AA . Part A is still visible on the next day in the Meudon spectrograph (Figure 1). Right panels: TRACE 171 \AA observations of the dark filament channel and fine filament structures seen as absorption feature (c) on 25 August at 13:04 UT and (d) on 26 August at 06:05 UT. The fine structures are indicated by black arrows. The continuous line underlines the filament spine. The dashed line indicates the median line of the filament channel. Notice the increasing distances between these two lines between 25 August and 26 August, indicating the slow rise of the filament. Section C consists of a long bright thread indicating some heating on 26 August.

by dark regions. In Figure 4c, d we have drawn the contour of the filament spine and the median line of the filament channel. By comparing the images of 25 and 26 August we see clearly an increasing distance between these two lines.

Following the evolution we can give some quantitative values: its projected altitude is estimated at around 30 000 km on 25 August at 13:04 UT, and 75 000 km on 26 August at 06:05 UT. On 25 August the filament altitude increased by 35 arc sec in six to nine hours, which is equivalent to a rising velocity of 1 km s^{-1} , not taking into account some perspective effects; thus it is a minimal value.

On 26 August between 04:00 UT and 09:00 UT, the filament altitude increased again by 20 arc sec, which means that the velocity was still around 1 km s^{-1} . Finally, between 08:00 UT and 09:00 UT, there was an acceleration and the velocity reached 5 km s^{-1} , after which time the filament left the field-of-view of TRACE. These values are comparable to previous observations of filament eruption in quiet Sun (Schmieder *et al.*, 2000; Sterling and Moore, 2003).

4. Magnetic Field of the Filament Environment

The longitudinal magnetic field observed by MDI is shown in Figure 5 with a box representing the field-of-view of THEMIS/MTR. The corresponding $H\alpha$ MTR observation is presented in the OSPAN image. We remark that the fine structures in $H\alpha$ have a certain

Table 1 Table of THEMIS MTR observations (the step unit is 0.8 arc sec).

Date	Sequence	Time UT	Size of the image
23 August 2006	23	16:35 – 17:56	200 steps \times 0.8'' \times 74''
	25	18:07 – 19:00	100 steps \times 0.5'' \times 74''
24 August 2006	13	10:26 – 12:04	200 steps \times 0.8'' \times 74''
	14	14:20 – 15:58	idem
25 August 2006	2	11:13 – 12:34	150 steps \times 0.8'' \times 74''
26 August 2006	8	14:20 – 15:28	120 steps \times 0.8'' \times 74''
27 August 2006	4	10:48 – 12:20	

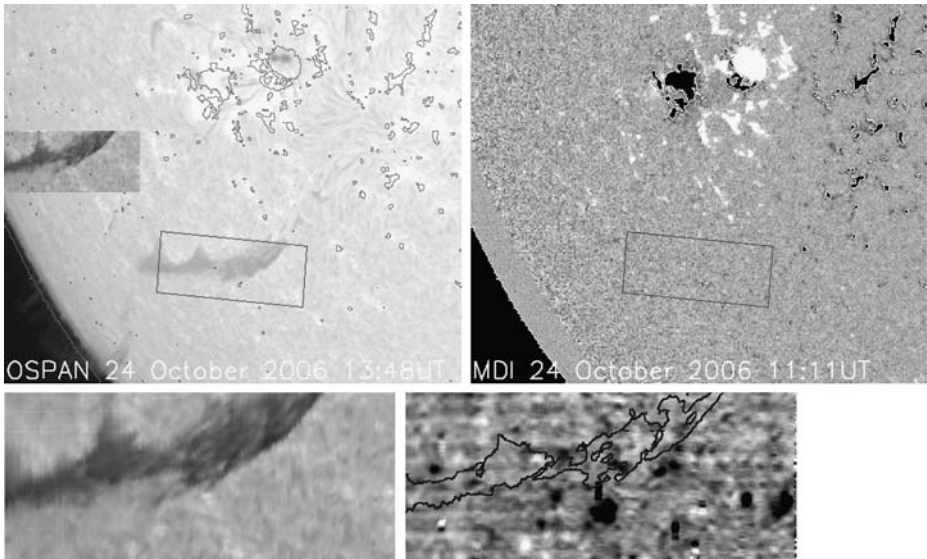


Figure 5 Top panels: Coalignment of THEMIS/MTR observations, OSPAN (top left) and MDI (top right) with MDI magnetic contours in both top panels (± 80 G) for 24 August 2006. The box represents the field-of-view of THEMIS; over the OSPAN image we have put a THEMIS $H\alpha$ image at the same scale. Bottom panels: THEMIS observations (bottom left) in $H\alpha$, (bottom right) saturated (± 30 G) magnetic strength overlaid by $H\alpha$ contours (thick black contours).

angle with the filament axis on 24 August (around 30 degrees) which is reduced to zero on 25 August (Figure 2).

The MDI movie shows very weak and intermittent polarities in the filament channel. It is difficult to identify canceling flux using low-resolution data of MDI. THEMIS, with its high polarimetric sensitivity, allows us to detect with confidence weaker polarities (Figure 5) (López-Ariste *et al.*, 2006; Schmieder *et al.*, 2006). All the polarities overlaid by contours in the MTR magnetic flux map have good Stokes parameter profiles. But THEMIS has one or two observations per day of this region and the time evolution of such weak polarities is too fast to be studied with so few data.

THEMIS/MTR observed the filament on 24 August (sequence 13) and on 25 August (sequence 2) between 11:13 UT and 12:34 UT (150 steps of 0.8 arc sec, the pixel size along the slit is 0.24 arc sec) (Figure 6). The polarimetric signal was recorded with the

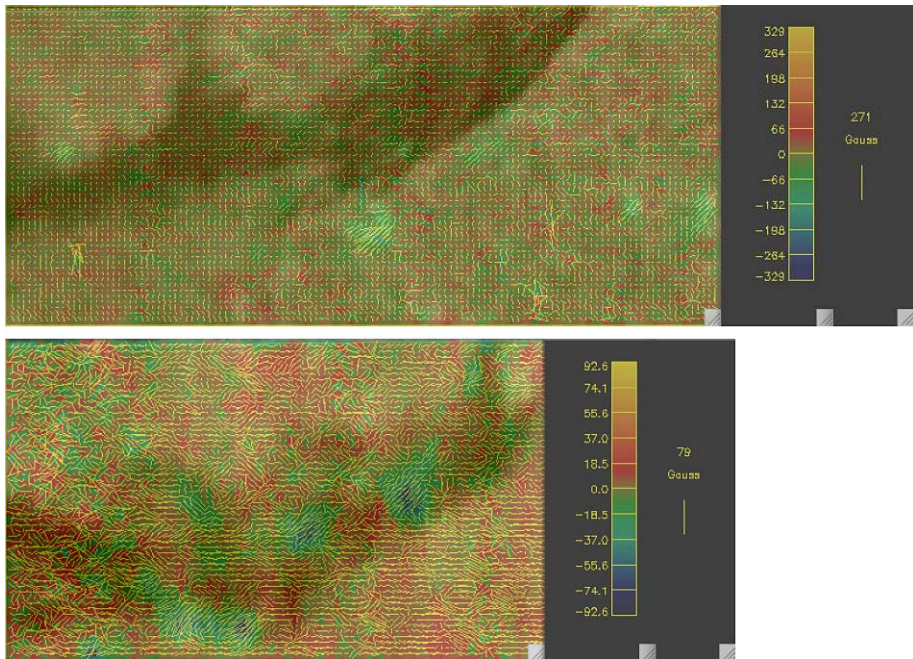


Figure 6 THEMIS H α filament and superimposed the vector magnetic map for 24 August between 10:26 and 12:04 UT (upper panel) and 25 August between 14:20 and 15:28 (lower panel). The H α filament overlays the negative polarities on 25 August because of its increasing height. The longitudinal magnetic field is drawn with colors (warm colors – yellow, red – for the field going out of the Sun, cold colors – blue, green – for the field entering the Sun). The transverse field is drawn having a proportional length, without an arrow because the 180-degree ambiguity is not solved. See Figure 5 for the field-of-view of 24 August (160 arc sec \times 74 arc sec). The field-of-view of 25 August is slightly shifted towards the southeast and smaller (120 arc sec \times 74 arc sec). The x axis is along the scan, the y axis is along the slit. The scale for magnetic fields on 24 August is ± 330 G, and on 25 August is ± 80 G.

beam exchange technique. On 26 August, the observations were done around 14:20 UT. The filament was not well visible, only the east part remained, and on the 27 August we did not see the filament.

The total magnetic field strength of the network surrounding the filament channel is presented in Figure 7. The maximum values fell between 24 August and 25 August from 400 G to 100 G. Well-identified polarities in the filament channel decreased from 200 G to 50 G (Figure 7). The mean value of the total magnetic field decreased from 38 G on 24 to 27 August G on 25–26 August with a threshold of 20 G to eliminate the noise, the mean longitudinal magnetic field also decreased from 32 G to 24 G. The projection effect should increase the value of the magnetic field. In order to confirm the general decrease of the magnetic field in the environment of the filament, we computed the total flux using MDI data in a large area (450 \times 160 arc sec). Taking into account the increase of the area surface during the three days (24 to 26 August) due to its approach to the central meridian and the differential rotation, we found the following values: 1.7×10^{21} Mx, 1.5×10^{21} Mx and 1.4×10^{21} Mx, respectively for 24 to 26 August. The network had less and less strong polarities that cannot be explained by the dispersion of the magnetic field, the total flux being decreasing.

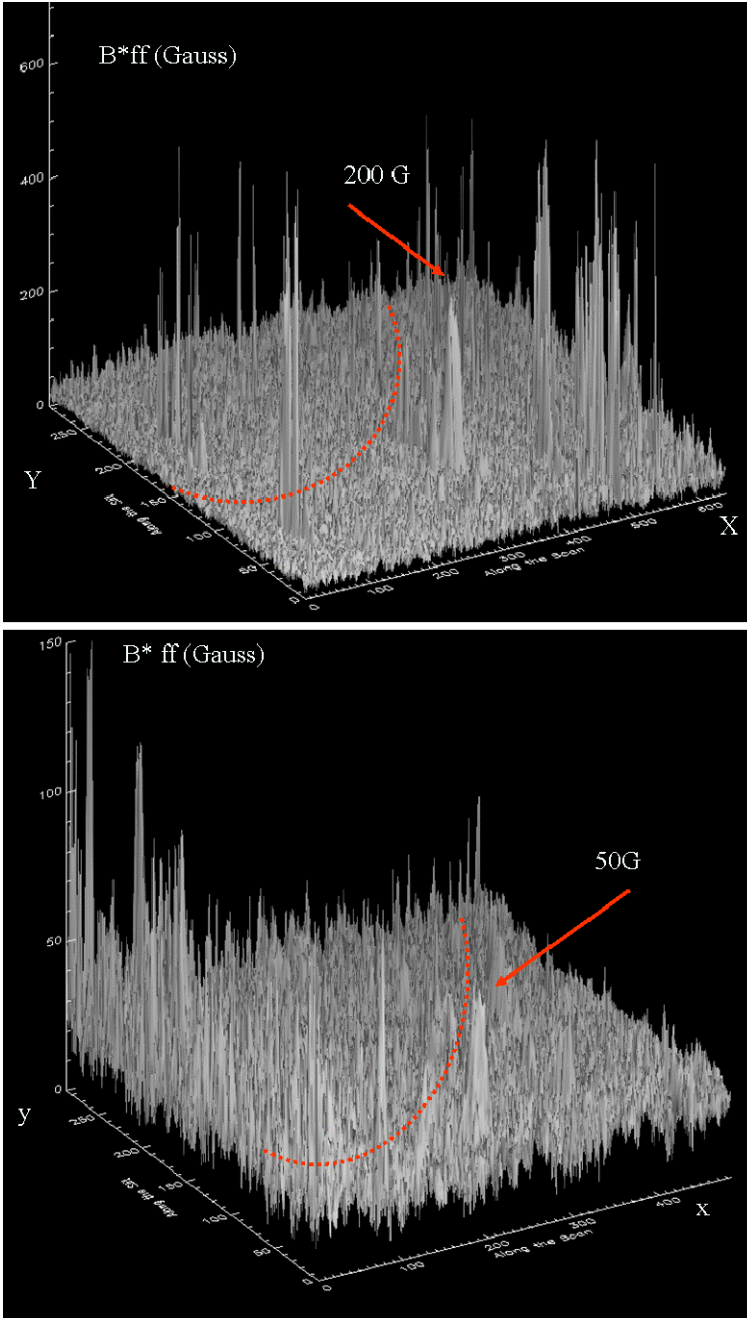


Figure 7 3D map of the background magnetic field strength of the filament measured in the Fe I doublet 6102 \AA from THEMIS observations corresponding to the vector magnetic field maps of Figure 6. Top panel: on 24 August; bottom panel on 25 August. The dashed lines represent the main filament axis. The arrows indicate some maxima of the field strength corresponding to network polarities.

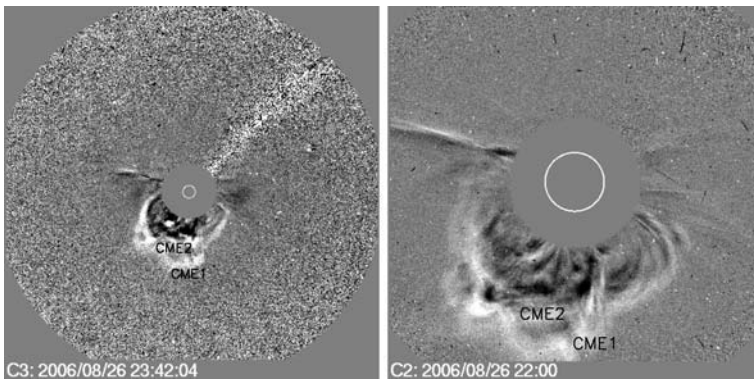


Figure 8 Complex CME observed by LASCO with C2 (right panel) and C3 (left panel) due to the eruption of the filament and a C2.5 flare. The two expected CMEs are noted CMI and CM2.

5. LASCO CME

LASCO reported on the observations of 26 August 2006 as follows: the CMEs occurred in two phases. At 09:00 UT in the SE (south, east), a very narrow (jet-like) loop front was observed. Then, at 10:00 UT in the SSW (south, southwest), a system of very faint loop fronts slowly developed (Figure 8). It is nevertheless difficult to give an exact time of first appearance. At 20:48 UT, in the SSE (south, southeast), diffuse brightenings formed a Partial Halo Event.

Two Partial Halos can be distinguished with two different structures: *i*) a very bright and expanding loop front developing mainly toward SSE [CME 1], and *ii*) a ragged and wider loop front developing toward S, slightly behind [CME 2]. CME 1 is first seen in C3 at 21:42 UT appearing on SSE, then developing as a bright and ragged loop front, while CME 2 shows up above the S Pole by 22:18 UT. The mean plane-of-sky speed of the outermost front of the event (CME 1) at PA 170° was 730 km s^{-1} (based on C3 data). As for CME 2, the mean plane-of-sky speed of its LE at PA 172° was 585 km s^{-1} . GOES reported a C2.5 X-ray flare on NOAA AR 10905 (S11E10) between 19:52–20:32 UT with peak emission at 20:07 UT. In summary, LASCO concludes that the event is a Partial Halo Event, front-sided, associated with the C2.5 X-ray event in AR 10905 (see images and movies of the event in the web pages given at the end of the paper) or in <ftp://ares.nrl.navy.mil/pub/lasco/halo/20060826>.

We propose a different interpretation. CME 1 could be due to the eruption of the large filament, identified as a slow CME and accelerated later by CME 2 related to the C2.5 flare. If so, it means that the launch of the CME would be around 9 to 10 UT, visible at 21:42 UT at four solar radii. This indicates a velocity of the order of 100 km s^{-1} or even less, before being pushed by CME 2. The other possibility is that the eruption did not launch a CME at all. In the latter case it would mean that the material disappears by counter-streaming during the rise of the magnetic field lines and explains the partial disappearance of part B of the filament. We have no observations in $\text{H}\alpha$ nor in EUV after 9 UT. The two solutions may coexist. The TRACE images later in the day do not show the reformation of the part B of the filament neither it is seen in $\text{H}\alpha$ on the next day.

6. Conclusions and Discussion

The main conclusions are the following. Counter-streaming in an activated filament was observed more than 24 hours before eruption, and some changes of orientation of the H α fine structures in the filament body were detected. The photospheric magnetic field strength in the network surrounding the filament channel was strongly decreasing during two days before the eruption. The eruption of the filament is suspected to be the onset of a slow CME observed by LASCO.

Due to the decreasing magnetic field strength, the filament globally rose with material flowing in both directions. The filament had longer fine structures and fewer footpoints. This implies that the field lines no longer had dips but became loop-like. The material along the field lines had a counter-streaming activity. The flux tube rose slowly for 24 hours and accelerated during the last hour before its eruption. We could expect that the consequent CME occurred with a very slow velocity (100 km s^{-1}) according to our interpretation of the LASCO observations. This slow CME would be merged with a faster one generated by a flare occurring ten hours later in the active region belonging to the same magnetic system (Figure 1). Such a slow CME has previously been detected after filament eruption (Schmieder *et al.*, 2000). The filament is not reformed after its eruption. We did not detect canceling flux, neither small-scale brightenings in H α , nor in TRACE 195 Å. Therefore the classical “tether cutting” mechanism (Moore and Roumeliotis, 1992) cannot take place in this magnetic structure. We also found no evidence of coronal reconnection above the filament which would support a breakout mechanism (Antiochos, DeVore, and Klimchuk, 1999).

Simulations of prominence eruption, however, show the importance of the photospheric boundary conditions. Amari *et al.* (1999) modeled a prominence by producing a configuration consisting of a twisted magnetic flux embedded in an overlying, almost potential, arcade such that high electric currents are confined in the tube. This tube is formed by gradual photospheric diffusion processes. When this process lasts for a long enough time, Amari *et al.* (2000) showed that the magnetic configuration cannot stay in equilibrium so that it leads to a CME. Photospheric diffusion should not produce significant H α emission, therefore this mechanism may be active in this event. However, we are in a magnetic configuration where there is no a priori magnetic reconnection in the low photosphere: indeed, we could not detect canceling flux in the photosphere. But in fact the noise was very large that far from disk center with MDI and the temporal resolution was too coarse with THEMIS.

Acknowledgements The Optical Solar Patrol Network (OSPAN) project is a collaboration between the Air Force Research Laboratory Space Vehicles Directorate and the National Solar Observatory. OSPAN was formerly known as ISOON, the Improved Solar Observing Optical Network; its name was changed in 2006. THEMIS is a French-Italian telescope operating in the Canary Islands. We thank G. Aulanier for fruitful discussions on possible mechanisms of filament destabilization. We deeply thank the anonymous referee for his/her very constructive remarks that improved the paper.

References

- Amari, T., Luciani, J.F., Mikic, Z., Linker, J.: 2000, *Astrophys. J.* **529**, L49.
 Amari, T., Luciani, J.F., Mikic, Z., Linker, J.: 1999, *Astrophys. J.* **518**, L60.
 Antiochos, S.K., DeVore, C.R., Klimchuk, J.A.: 1999, *Astrophys. J.* **510**, 495.
 Anzer, U., Heinzel, P.: 2005, *Astrophys. J.* **622**, 714.
 Aulanier, G., Démoulin, P.: 1998, *Astron. Astrophys.* **329**, 125.
 Bommier, V., Landi Degl’Innocenti, E., Landolfi, M., Molodij, G.: 2007, *Astron. Astrophys.* **464**, 323.
 Démoulin, P.: 2007, *Adv. Space Res.* **39**, 11. 1674.

- Démoulin, P., Vial, J.C.: 1992, *Solar Phys.* **141**, 289.
- Dudík, J., Aulanier, G., Schmieder, B., Bommier, V.: 2007, *Solar Phys.*, submitted.
- Falconer, D.A.: 2001, *J. Geophys. Res.* **106**(A11), 25185.
- Falconer, D.A., Moore, R.L., Porter, J.G., Gary, G.A., Shimizu, T.: 1997, *Astrophys. J.* **482**, 519.
- Isenberg, P.A., Forbes, T.G., Démoulin, P.: 1993, *Astrophys. J.* **417**, 368.
- Handy, B.N., et al.: 1999, *Solar Phys.* **187**, 229.
- Hindman, B.W., Haber, D.A., Toomre, J.: 2006, *Astrophys. J.* **653**, 725.
- Kuin, N., Paul, M., Martens, P.: 1986, In: Poland, A. (ed.) *CPP Workshop Proceedings, NASA 2442*, 241.
- Lin, J.: 2004, *Solar Phys.* **219**, 169.
- Lin, J., Forbes, T.G.: 2000, *J. Geophys. Res.* **105**, 2375.
- Lin, J., Forbes, T.G., Isenberg, P.A.: 2001, *J. Geophys. Res.* **106**, 25053.
- Lin, Y.L., Wiik, J.E., Engvold, O.: 2003, *Solar Phys.* **216**, 109.
- Lin, Y.L., Wiik, J.E., Engvold, O., Rouppe van der Voort, L., Frank, Z.A.: 2005, *Solar Phys.* **227**, 283.
- López-Ariste, A., Aulanier, G., Schmieder, B., Sainz Dalda, A.: 2006, *Astron. Astrophys.* **456**, 725.
- Low, B.C.: 2001, *J. Geophys. Res.* **106**, 25141. 1122.
- MacKay, D.H., van Ballegooijen, A.A.: 2006, *Astrophys. J.* **643**, 577.
- Mein, N., Schmieder, B., DeLuca, E., Heinzel, P., Mein, P., Malherbe, J.M., Staiger, J.: 2001, *Astrophys. J.* **556**, 438.
- Moore, R.L., Roumeliotis, G.: 1992, In: Svestka, Z., Jackson, B.V., Machado, M.E. (eds.) *IAU 133*, Springer, New York.
- Mouradian, Z., Martres, M.J., Soru-Escaut, I.: 1986, In: Poland, A. (ed.) *CPP Workshop Proceedings, NASA 2442*, 221.
- Rondi, S., Roudier, T., Molodij, G., Bommier, V., Keil, S., Sütterlin, P., Malherbe, J.M., Meunier, N., Schmieder, B., Maloney, P.: 2007, *Astron. Astrophys.* **467**, 1289.
- Schmieder, B., van Driel-Gesztelyi, L.: 2005, In: Dere, K., Wang, J., Yan, Y. (eds.) *Coronal and Stellar Mass Ejections, IAU Symp. 226*, Cambridge Univ. Press, Cambridge, 149.
- Schmieder, B., Delannée, C., Deng, Y.Y., Vial, J.C., Madjarska, M.: 2000, *Astron. Astrophys.* **358**, 728.
- Schmieder, B., van Driel-Gesztelyi, L., Aulanier, G., Démoulin, P., Thompson, B., de Forest, C., Wiik, J.E., Saint Cyr, C., Vial, J.C.: 2002, *Adv. Space Res.* **29**, 1451.
- Schmieder, B., Lin, Y., Heinzel, P., Schwartz, P.: 2004, *Solar Phys.* **221**, 297.
- Schmieder, B., Aulanier, G., López Ariste, A., Mein, P.: 2006, *Solar Phys.* **238**, 245.
- Sterling, A., Moore, R.: 2003, *Astrophys. J.* **599**, 141.
- Subramanian, P., Dere, K.D.: 2001, *Astrophys. J.* **561**, 372.
- Švetska, Z.: 1986, *The Lower Atmosphere of Solar Flares*, NSO/Sac Peak Pub., 332.
- Török, T., Kliem, B., Titov, V.S.: 2004, *Astron. Astrophys.* **406**, 1043.
- Wang, J.X.: 2002, In: Hénoux, J.C., Fang, C., Vilmer, N. (eds) *Second French–Chinese Meeting*, World Publishing, 145.
- Zirker, J.B., Engvold, O., Martin, S.F.: 1998, *Nature* **396**, 440.
- Zhou, G.P., Wang, J.X., Cao, Z.L.: 2003, *Astron. Astrophys.* **397**, 1057.